

Multiple localized-itinerant dualities in magnetism of 5f electron systems. The case of UPt_2Si_2

L. M. Sandratskii^{1,2*}, V. M. Silkin^{2,3,4}, L. Havela⁵

¹*Institute of Physics, Czech Academy of Sciences, 182 21 Prague, Czech Republic*

²*Donostia International Physics Center (DIPC),*

Paseo de Manuel Lardizabal 4, E-20018 San Sebastián, Spain

³*Departamento de Polímeros y Materiales Avanzados: Física,*

Química y Tecnología, Facultad de Ciencias Químicas,

Universidad del País Vasco (UPV-EHU), Apdo. 1072, E-20080 San Sebastián, Spain

⁴*IKERBASQUE, Basque Foundation for Science, 48011 Bilbao, Spain*

⁵*Faculty of Mathematics and Physics, Charles University, 12116 Prague, Czech Republic*

The paper deals with the U based compound UPt_2Si_2 (UPS). The material was first treated as a localized 5f-electron system. Later, an opposite opinion of a predominantly itinerant nature of the system was put forward. The most recent publications treat UPS as a dual material. We suggest a material specific theoretical model based on the density functional theory plus Hubbard U (DFT+ U) calculations that describes the set of fundamental ground-state properties and high magnetic field experiment. The ground state properties include antiferromagnetic magnetic structure, magnetic easy axis, and the value of the U atomic moment. The in-field experiment shows the presence of a strong metamagnetic transition for the field parallel to the easy axis in contrast to the hard field direction where such a feature is absent. On the other hand, comparable induced magnetization values are obtained for both easy and hard field directions. Within the framework of the suggested model we show that the compound possesses well-formed atomic moments built by electrons treated as delocalized. To understand the experimental high-field properties we estimate exchange energy, magnetic anisotropy energy, and Zeeman energy. All three energies are shown to have comparable values what is crucial for the interpretation of the experiment. At all steps of the study we devote special attention to revealing and emphasizing the dual itinerant-localized properties of the material. The obtained forms of the duality are different: well defined atomic moments formed by the itinerant electrons, interplay of the single-site and two-site anisotropies, strong localization of two of the 5f electrons in contrast to the itinerant nature of the 5f electrons contributing to the states around the Fermi level, intense Stoner continuum competing with spin wave formation. The obtained high sensitivity of the calculated properties to the details of the theoretical model reflects the complexity of the multi-orbital 5f electron system. The latter is the origin of the wide range of complex behavior observed in U based materials.

PACS numbers:

I. INTRODUCTION

The magnetic properties of the U-based compounds are highly diverse (see, e.g., some reviews and recent publications 1–12). The magnetic structures of the materials vary widely including ferromagnetism (FM), antiferromagnetism (AFM), spin-density waves (SDW), noncollinear commensurate and chiral incommensurate structures. Besides the rich variety of ground state properties one finds numerous metamagnetic transitions (MMTs) whose features depend on the direction of applied magnetic field. In spite of a vast amount of collected experimental and theoretical knowledge, the understanding of the U-based compounds is far from complete.

The complexity of the properties of the U based materials led to the suggestion of a variety of physical models different in their key assumptions. Some models treat the U 5f electrons and U magnetic moments as local-

ized and the physics of the materials as dominated by the processes characteristic for isolated atoms. To the localized-type properties belong, for example, the atomic magnetic moments formed according to the Hund's rules and many-electron atomic multiplets. Other models emphasize the itinerant nature of the 5f magnetic moments and the participation of the 5f orbitals in the formation of the Fermi surface (FS). As can be expected in such a situation, there also exist dual models stressing coexistence of both localized atomic-like and collective itinerant features in the same U based material.

The complexity characteristic for the U based systems is clearly manifested in the case of UPt_2Si_2 (UPS), the compound that constitutes the topic of the present study. In recent years, UPS attracted considerable research attention and was identified as the material with dual nature of magnetism. Looking at a longer time frame, we find that UPS was first treated as a localized-electron magnet¹³. In later publications it was suggested that the system is predominantly itinerant^{14,15}. In Ref. 16, a dual theoretical treatment of the 5f electrons was reported. The duality became the title property of UPS in Ref. 17

*lsandr3591@gmail.com

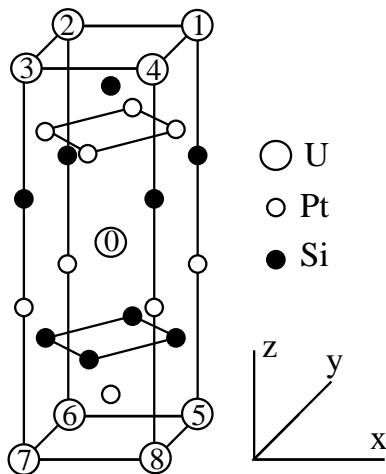


FIG. 1: Crystal structure of UPS. The z axis corresponds to the crystallographic c axis. The x axis corresponds to the crystallographic a axis. The numbering of the U atoms is used in the symmetry analysis performed in Sec. IV C 2.

though the duality concept here is different from that in Ref. 16. Also in the most recent publication¹⁸ dealing with charge density wave, the material is characterized as dual magnet.

The experimental information about fundamental magnetic properties of UPS is the following. The material has ferromagnetic U layers that are antiferromagnetically coupled to each other (Fig. 1). The easy axis is orthogonal to the ferromagnetic layers. The large U moments up to $2.5 \mu_B$ were reported¹⁹. The high magnetic field experiment¹⁵ shows strong dependence of the magnetic response on the direction of applied field. For $B \parallel z$ there is a distinct MMT while for $B \parallel x$ such a clear feature is absent. At the same time, large induced magnetizations of comparable values 1.5 and $1.1 \mu_B/\text{U}$ are obtained in maximal field of ~ 50 T for, respectively, easy and hard field directions. While early in-field experiments were interpreted in terms of localized model, in Ref. 15 the itinerant model and major role of the Lifshitz transition were proposed^{20,21}. Interesting results of the inelastic neutron scattering (INS) measurements were reported in Ref. 17. They have shown the presence of local U moments involved in transversal fluctuations coexisting with the absence of any signature of spin wave excitations.

The material-specific density-functional-theory (DFT) based theoretical studies of the magnetic properties of UPS are scarce^{14,16}. In Ref. 14, the authors report the comparison of the AFM and FM energies obtained in the local density approximation (LDA) that agrees with the experimental situation. The atomic U moment is calculated with three methods: LDA, LDA plus orbital polarization correction²² (LDA+OPC) and LDA+ U ²³. As expected, the LDA result underestimates the value of the U atomic moment giving $0.71 \mu_B$. This DFT weakness has been understood quite a time ago as the consequence

of the underestimation of the orbital moment²². The DFT+OPC method was suggested and intensively used to improve on this issue. This method was directly designed to increase the value of the orbital moment (OM) by introducing an effective orbital magnetic field²². In Ref. 14, the use of the DFT+OPC method with a selected effective field parameter resulted in an increased total moment of $2.06 \mu_B$. The DFT+ U method has a more solid theoretical basis and has the ability, through introducing orbital dependent potentials, to solve the problem of the OM underestimation²⁴. Rather unexpected, the application of the LDA+ U method in Ref. 14 resulted in a further reduction of the OM that became even smaller than the spin moment. The FS was calculated and the conclusion about predominantly itinerant nature of the 5f electrons was drawn. In Ref. 16 the theoretical study of the FS was continued with application of the dual approach where two of the 5f electrons are treated as localized and the rest of the 5f electrons as itinerant.

The purpose of the present paper is a systematic material-specific study of UPS aiming at obtaining the theoretical model providing the agreement with experiment for the set of fundamental magnetic properties: the type of magnetic structure, the character of magnetic anisotropy (MA), the value of atomic moments. The model thus gained is applied to the interpretation of the high magnetic-field experiment. A possible microscopic reason of the absence of spin waves, as detected in the INS experiment, is also briefly addressed.

Our study is based on the DFT and DFT+ U calculations for a number of magnetic configurations. Special attention is given to the analysis of the calculation results from the viewpoint of the interplay of localized and delocalized properties of the 5f electron system. In particular, we relate the physical picture following from our calculations to the dual model of two separate groups of the 5f electrons applied to UPS in Ref. 16. For some U_H values, we obtain and discuss the violation of the Bruno's relation²⁵⁻²⁷ between magnetic anisotropy energy (MAE) and OM anisotropy (OMA). (In the following we will use U_H as the notation for the Hubbard parameter to easier distinguish it from the chemical symbol for uranium.)

The paper is structured as follows. In Sec. II the relevant forms of localized-itinerant dualities are discussed. Section III is devoted to the method of calculation. In Sec. IV the results of the calculations are presented and discussed. The last section is devoted to the conclusions.

II. DUALITY FORMS

The analysis of the experimental results and theoretical models in terms of the itinerant-localized duality helps to gain a deeper understanding of the magnetic systems. The concrete forms of duality can be very different. Therefore it is worthwhile to devote this short section to a brief preliminary discussion of the duality forms relevant to our study.

The dual behavior is obtained already on the level of individual electron states. The DFT based treatment considers the 5f U orbitals as a part of the Bloch wave functions extended over whole crystal and, therefore, as a part of the delocalized electron picture. On the other hand, the spatial distribution of the 5f electron density within the crystal volume assigned to the U atoms resembles the 5f density distribution in isolated U atoms. This duality in the properties of individual electron states is the origin of other duality types.

Historically, the understanding of the role of duality concept was crucial for solving the long-lasting conflict between localized and itinerant approaches to the classical 3d magnets²⁸⁻³⁰. The solution of this contradiction was found in recognizing that the itinerant electrons can build well-formed atomic moments participating in local transversal magnetic fluctuations. On this basis it is possible to employ the DFT calculations for mapping an itinerant electron system with well-formed atomic moments onto the Heisenberg Hamiltonian³¹⁻³⁵.

There is a straightforward DFT-based method to examine if well-formed atomic moments are present in a given material. It consists in carrying out self-consistent calculations of various magnetic configurations. If such calculations converge to the magnetic states with close values of atomic moments the picture of well-defined atomic moments is justified. We will apply this method to UPS.

Another aspect of the dual nature of the 5f electron systems is the fact that the DFT methods often do not provide an accurate enough description of the intraatomic 5f electron correlations. Among the methods to improve on this is the DFT+ U method²³. We will employ both DFT and DFT+ U methods.

An important aspect of the physics of the U based materials is the multi-orbital nature of the 5f electron system. A special form of the dual treatment of the U compounds was suggested^{36,37} that consists in different treatment of the 5f electrons occupying different orbitals: Two electrons are treated as localized and not hybridizing with other electron states whereas the rest of the 5f electrons is treated as itinerant. We will refer to this form of duality as two-5f-electron-groups (T5FEG) duality. This duality treatment was applied to UPS in Ref. 16. This approach was successfully used in the study of a series of UM_2Si_2 ($M=Pd, Ni, Ru, Fe$) compounds³⁸. We will relate the results of our calculations to the assumptions of the T5FEG-duality approach.

III. METHOD OF CALCULATION

The calculations are performed with the augmented spherical waves (ASW) method^{39,40} generalized to deal with spin-orbit coupling (SOC)⁴¹. The generalized gradient approximation (GGA) to the energy functional⁴² is employed in the calculations. The DFT+ U method in the form suggested by Dudarev *et al.*⁴³ was applied

to examine the influence of the on-site correlation of the U 5f electrons on the magnetic moments and energies of the magnetic configurations. The most of calculations were performed with \mathbf{k} -mesh $20 \times 20 \times 20$. This allowed to reach the convergence of the energy differences between magnetic configurations of 0.01 mRy per U atom.

An important quantity of the DFT+ U approach is the orbital density matrix n of the correlated atomic states. It enters the method with the prefactor U_H leading to the orbital dependence of the electron potential⁴³

$$V_{m,m'}^{s,s'} = -U_H(n_{m,m'}^{s,s'} - \frac{1}{2}\delta_{m,m'}\delta_{s,s'}). \quad (1)$$

In the paper we work in the basis of complex spherical harmonics Y_{lm} . The orbital dependence of the potential is given by the dependence on the magnetic quantum number m . The diagonal elements $n_{m,m}^{s,s}$ of the orbital density matrix give the occupations of the orbitals corresponding to quantum numbers m and spin projections s .

We calculate the vectors of spin \mathbf{m}_s^ν and orbital \mathbf{m}_o^ν moments of the ν th atom as

$$\mathbf{m}_s^\nu = \sum_{\mathbf{kn}}^{occ} \int_{\Omega_\nu} \psi_{\mathbf{kn}}^\dagger \boldsymbol{\sigma} \psi_{\mathbf{kn}} d\mathbf{r} \quad (2)$$

$$\mathbf{m}_o^\nu = \sum_{\mathbf{kn}}^{occ} \int_{\Omega_\nu} \psi_{\mathbf{kn}}^\dagger \hat{\mathbf{l}} \psi_{\mathbf{kn}} d\mathbf{r} \quad (3)$$

where $\boldsymbol{\sigma} = (\sigma_x, \sigma_y, \sigma_z)$ is the vector of Pauli matrices and $\hat{\mathbf{l}} = (\hat{l}_x, \hat{l}_y, \hat{l}_z)$ is the operator of orbital angular momentum, $\psi_{\mathbf{kn}}$ is the wave function of the Kohn-Sham state corresponding to wave vector \mathbf{k} and band index n . The sum is taken over occupied states. The integrals are carried out over ν th atomic sphere.

Due to the orbital-dependent potential term [Eq. (1)] the occupied orbitals tend to lower their energies whereas empty orbitals tend to increase their energies. This feature makes the DFT+ U approach an adequate tool for the study of the enhancement of the orbital magnetic moment²⁴. We will study the dependence of the selected fundamental properties on U_H aiming at obtaining the model describing the experimental results.

The elements of the n matrix determine the value of the OM⁴⁴. The z component of the OM, m_{oz} , is determined by the diagonal elements

$$m_{oz} = \sum_s \sum_{m=-3}^3 m n_{m,m}^{s,s} = \sum_s \sum_{m=1,2,3} m (n_{m,m}^{s,s} - n_{-m,-m}^{s,s}). \quad (4)$$

We will perform calculations for four magnetic configurations: two AFM and two FM structures with moments parallel to the z and x axes. The configurations will be labeled as AFM $_Z$, AFM $_X$, FM $_Z$, and FM $_X$.

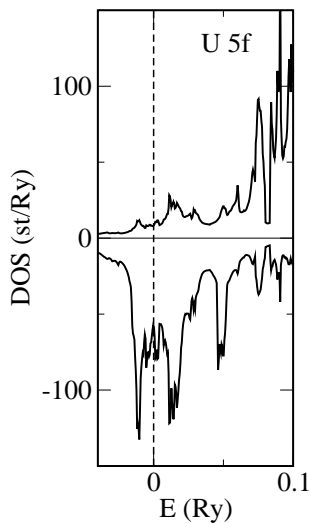


FIG. 2: Spin projected U 5f DOS for the AFM_Z configuration. GGA calculation.

In the projection of the quantities on an axis we will always chose the direction of the axis parallel to the direction of the total moment. Therefore the projection of the orbital moment will be positive, and the projection of the spin moment will be negative. Accordingly, the majority spin occupation corresponds to the electron states with negative spin projection.

IV. RESULTS AND DISCUSSION

A. The results of the GGA calculations

TABLE I: Energies and U magnetic moments for four magnetic configurations calculated with the GGA potential. m_s , m_o and m_t are the values of spin, orbital and total moments in units of μ_B . The directions of the spin and orbital moments are opposite to each other. The direction of the total moment is parallel to the direction of the orbital moment.

	E (mRy/U)	m_s	m_o	m_t
AFM _Z	0	1.92	2.77	0.85
AFM _X	0.54	1.93	2.68	0.75
FM _Z	0.59	1.78	2.75	0.97
FM _X	1.27	1.79	2.62	0.83

We begin with the discussion of the results of the GGA calculations. The values of the energies and U magnetic moments are collected in Table I. In agreement with experiment, the ground state magnetic configuration is AFM_Z. Therefore, both the AFM magnetic structure and the easy c axis are captured correctly. The total U moment of $0.85 \mu_B$ is, as expected, too small.

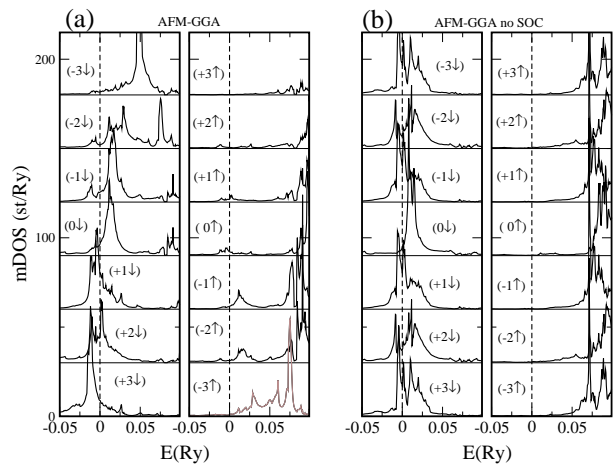


FIG. 3: m and spin projected U 5f DOSs for the AFM_Z configuration. (a) The GGA calculation with SOC taken into account. (b) The GGA calculation without SOC.

In Fig. 2 we show the spin projected U 5f DOSs for the AFM_Z configuration. The origin of the spin moment is well seen: The spin splitting of the states and, as a consequence, different occupation of the spin-up and spin-down 5f orbitals determines the value of the spin moment. However, the spin-projected DOSs provide no information on the origin and value of the OM. To visualize the formation of the OM we need m -resolved partial DOSs. They are presented in Fig. 3(a). We see that the occupation of the 5f orbitals corresponding to positive m values in the spin-down channel is much higher than the occupation of the orbitals corresponding to negative m values. This $\pm m$ polarization of the mDOSs is the origin of the orbital magnetic moments [see Eq. (4)]. To understand deeper the interplay between spin and orbital components of the atomic moment we performed the calculation of the AFM structure neglecting SOC. We obtained spin moment of $2.16 \mu_B$ and zero OM. Considering SOC-free mDOSs (Fig. 3(b)) we see strong spin polarization of the U 5f orbitals whereas the $\pm m$ polarization is absent. (A detailed discussion of the symmetry properties of the m projected DOSs and occupation matrices n can be found in Ref. 45).

Continuing the analysis of the GGA results (Table I) we notice that rather large atomic spin and orbital moments are obtained for all four magnetic configurations. The values of the corresponding moments in all configurations are relatively close to each other. This gives us the basis for the conclusion that the U magnetic moments in UPS can be characterized as rather well formed. On the other hand, the variation of the values of both spin and orbital moments between the configurations is not negligible and reflects the influence of interatomic interactions, in particular interatomic hybridization.

Concluding this section we remark that in the GGA calculations Bruno's relation connecting MAE and OMA is fulfilled: the easy axis corresponds to the direction with

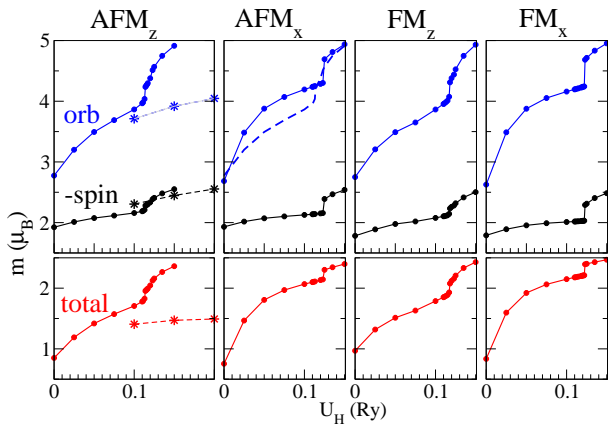


FIG. 4: The U_H dependence of the spin, orbital and total U magnetic moments for four magnetic configurations. The broken line in the AFM_X subgraph is the copy of the $m_o(U_H)$ dependence for the AFM_Z configuration. The asterisks in the AFM_Z subgraph show the data obtained in the T5FEG-model simulation (Sec. IV E).

a larger OM. In Sec. IV D we will see that in the GGA+ U calculations this relation is not obtained for some U_H values.

B. Results of the GGA+ U calculations

1. Atomic moments as functions of U_H

Since the GGA calculations underestimate substantially the value of the atomic moment, our next step is to carry out the GGA+ U calculations aiming at improved agreement with experiment in this respect. Of course the GGA+ U calculations change also the energies of the magnetic configurations. Therefore the question whether the AFM_Z configuration remains the lowest in energy is crucial for the realization of our goal to obtain the model describing the selected set of the properties.

In Fig. 4 we present the U_H dependence of the U moments for four magnetic configurations. Both spin and orbital moments for all configurations increase monotonously with increasing U_H . The OM grows faster than the spin moment leading to the monotonous increase of the total moment and improving agreement with experiment. For the AFM_Z configuration and $U_H > 0.12$ Ry the value of the total U moment exceeds $2 \mu_B$.

In Fig. 5, we show the mDOSs of the AFM_Z configuration calculated with $U_H = 0.1$ Ry. The comparison with the result of the GGA calculation shows that the energies of the $m = 3$ and $m = 1$ orbitals lie now distinctly below the Fermi level (E_F) and corresponding partial mDOSs are filled. The enhanced $\pm m$ polarization leads to the increase of the U OMs. To explain the difference in the U_H dependences of the spin and orbital moments we compare partial U 5f mDOSs obtained with GGA

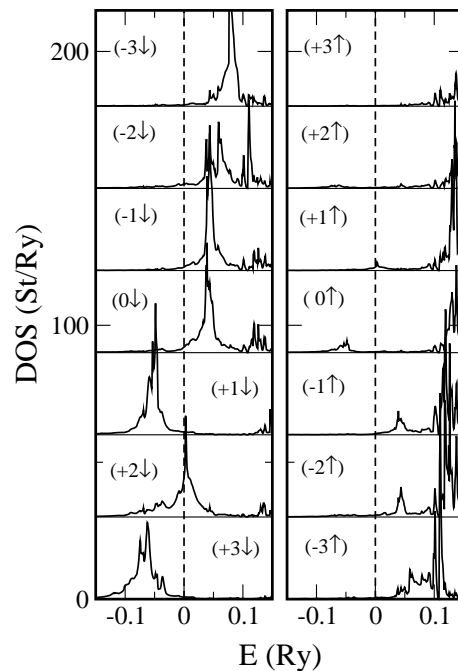


FIG. 5: The m and spin projected U 5f DOSs for the AFM_Z configuration calculated with GGA+ U method and $U_H = 0.1$ Ry.

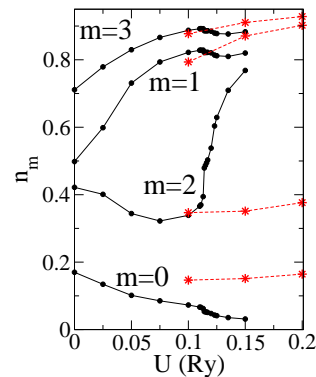


FIG. 6: The occupation numbers $n_m \equiv n_{m,m}$ for $m = 0, 1, 2, 3$ and spin-majority channel for the AFM_Z configuration. The data presented by asterisks will be discussed in relation with the simulation of the T5FEG model (Sec. IV E).

(Fig. 3) and GGA+ U (Fig. 5) calculations. As seen in Fig. 3, already for $U_H = 0$, the spin polarization of the 5f orbitals is large while their $\pm m$ -polarization is less manifested [Fig. 3(a)]. Although U_H tends to increase both polarizations, the large initial spin polarization limits its further increase.

Another feature obtained for all four magnetic configurations is the discontinuities in the $m(U_H)$ dependences at U_H values close to 0.12 Ry. The position of the singularity changes somewhat from case to case. To understand the nature of the discontinuous behavior we analyze in the case of the AFM_Z configuration the U_H depen-

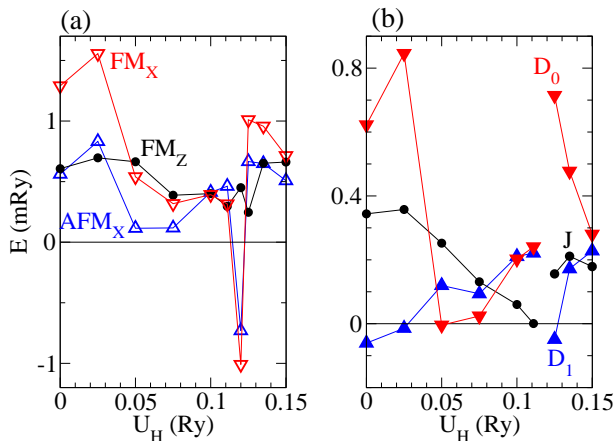


FIG. 7: (a) Energies of the AFM_X , FM_Z and FM_X configurations as functions of U_H counted from the energy of the AFM_Z configuration. (b) Parameters of the model Hamiltonian of interacting atomic moments as functions of U_H : isotropic exchange J , single-site anisotropy D_0 , two-site anisotropy (anisotropic exchange) D_1 .

dence of the occupation numbers $n_{m,m}$ for $m = 0, 1, 2, 3$ and the spin-majority channel (Fig. 6)⁴⁶. Obviously, the origin of the discontinuity is in the properties of the occupation number for $m = 2$. This is the U 5f orbital heavily present at the Fermi level. We remark that strong increase of the $m = 2$ occupation is accompanied by some decrease of other occupation numbers. The sum of the occupation numbers for all m and both spin projections changes from 2.52 for $U_H = 0.15$ Ry to 2.78 for $U_H = 0.1$ Ry.

In general, the shapes of the U_H dependences for corresponding moment types are rather similar in all four cases. This reveals that the formation of the moments is predominantly a local atomic effect while the change of the relative orientation of the atomic moments and their orientation with respect to the lattice have a smaller influence. Most importantly, the conclusion that UPS is the material with well-formed U atomic moments remains valid also in the GGA+ U calculations for all U_H values.

2. Energies of magnetic configurations as functions of U_H

In Fig. 7(a) we show the U_H dependence of the energies of the AFM_X , FM_Z and FM_X configurations counted from the energy of the AFM_Z configuration. We see that for all but one values of the U_H mesh the AFM_Z configuration is the lowest in energy. This means that the agreement with experiment concerning both the magnetic structure and the magnetic easy axis obtained for $U_H=0$ is a robust result preserved for most of the U_H values. At the same time, as we have seen in Sec. IV B 1, the use of the GGA+ U method improves the agreement with experiment concerning the value of the magnetic moment.

We suggest the following explanation of the deviating result for $U_H=0.12$ Ry. This U_H value lies in the region of the discontinuities in the U_H dependences of magnetic moments (Fig. 4). Importantly, it is above the discontinuity point for AFM_Z and below it for AFM_X and FM_X . Apparently, the comparison of the energies of two states, one of which is before and the other after the discontinuous transformation, can lead to the disagreement with experiment. The assumption that different states of the system are characterized by the same U_H value has been widely and successfully used. However, it does not have the status of a mathematically proven statement. Since the screening of the Coulomb interaction can change with the change of magnetic configuration, somewhat different U_H values should be expected for different configurations. In the region of the discontinuities this effect is expected to be enhanced.

We can summarize this issue as follows. Our analysis is focused on the trends in the U_H dependences. The comparison of the energies of different states of the system obtained with the same U_H value is a common practice proved to be reliable in many physical problems. In our case, we obtained agreement with experiment concerning both the magnetic structure and magnetic anisotropy for most of the U_H values. For the U_H values above the discontinuity points we have good agreement with experiment also in the value of the atomic moment. On the other hand, our results show that in the regions of discontinuous behavior an extra caution is required.

Continuing the analysis of the energy dependences $E(U_H)$ we notice that there are intersections of the functions corresponding to different magnetic configurations [Fig. 7(a)]. Since the energies of the magnetic configurations are determined by both exchange interaction and magnetic anisotropy, these results show that relative strength of the interactions varies with the variation of U_H . In particular, such a behavior shows that FM and AFM structures for some U_H values have different easy axes. This reveals the importance of the two-site anisotropy (anisotropic exchange). We will return to this issue in Sec. IV C 2 where the estimates of the anisotropy and exchange parameters are reported.

C. Interpretation of the in-field experiment

1. Experimental facts and general considerations

The high field magnetization measurements¹⁵ show that for the maximal applied magnetic field of 50 T the induced moments for $B||z$ and $B||x$ have comparable values of, respectively, $1.5 \mu_B$ and $1.1 \mu_B$ per U atom. These values, although large, are distinctly smaller than the ground-state atomic moments. The shapes of the $B||x$ and $B||z$ magnetization curves are very different. For the description of all details of the experimental curves we refer the reader to the original paper¹⁵ and review³. We will not attempt to theoretically reproduce

the experimental dependences in their full complexity. The main difference between the two experimental curves which we aim to understand is that for the $B||z$ field there is a strong increase of the magnetization by about $1 \mu_B$ in a relatively narrow field interval around 30 T revealing the presence of one or even two MMTs whereas in the $B||x$ case such a strong feature is absent.

This combination of properties reflects a certain relation between the interatomic exchange energy, magnetic anisotropy energy and in-field Zeeman energy. We will estimate corresponding energy scales and relate our estimations to the experimental situation. Since the calculations have shown the presence of well-formed atomic moments (Sec. IV B 1) our interpretation of the high field experiment considers the reorientation of the atomic moments as predominant factor.

It is worthwhile to briefly discuss the limiting cases where one of the three competing energy contributions is distinctly dominating. (i) If the AFM exchange interaction is dominant, a considerable distortion of the AFM structure cannot take place and a large induced magnetization is not expected for any field direction. (ii) If the MAE is dominant, the large induced moment for $B||x$ is not possible. For field $B||z$ exceeding the strength of the exchange interaction, the discontinuous spin-flip transition to the field-induced ferromagnetic state parallel to the z axis is expected. In this spin-flip state the moment per U atom would exceed $2 \mu_B$ that is larger than the observed value of the induced moment. (iii) If the Zeeman energy dominates, the spin-flip transition to the field-induced ferromagnetism is expected for any field direction.

All these limiting scenarios do not agree with experimental observations where large induced moments are obtained for both field directions and the induced moments are smaller than atomic moments. Therefore, the conclusion is that we deal with an interplay of different interactions having comparable energy scales⁴⁷. In Sec. IV C 2 we report an estimation of the scales of the exchange energy, MAE, and Zeeman energy (see Secs. IV C 2, IV C 3).

2. Calculation of exchange interaction and magnetic anisotropy parameters

The available energies of four magnetic configurations give three energy differences and allow us to perform an estimation of three interaction parameters of the model Hamiltonian of interacting atomic moments

$$H = \sum_{ij} \hat{\mathbf{S}}_i A^{(i,j)} \hat{\mathbf{S}}_j^T \quad (5)$$

where $A^{(i,j)}$ are 3×3 interaction matrices, T means matrix transposition, $\hat{\mathbf{S}}_i$ is the unit vector in the direction of the i th atomic moment. To do the parameter estimation efficiently it is important to perform the symmetry analysis of the $A^{(i,j)}$ matrices. If the SOC is not taken into account, the matrices have the scalar form

$$J \begin{pmatrix} 1 & 0 & 0 \\ 0 & 1 & 0 \\ 0 & 0 & 1 \end{pmatrix} \text{ which reflects the isotropic character of in-}$$

teratomic exchange interactions and the absence of magnetic anisotropy. In the relativistic case, only the hermiticity of the matrices is guaranteed by the general principles. The lattice symmetry imposes further restrictions on the form of the matrices. If $\{\alpha|\tau_\alpha\}$ is the symmetry operation of the lattice consisting from rotation α and translation τ_α , it imposes the following constraint on the interaction matrices

$$A^{(i,j)} = \alpha^T A^{(i_\alpha, j_\alpha, \mathbf{R})} \alpha \quad (6)$$

where the U sublattices i_α , j_α and lattice vector \mathbf{R} are defined by the action of operation $\{\alpha|\tau_\alpha\}$ on positions of atoms i and j (see Ref. 48 for the detailed description).

The crystal lattice of UPS is characterized by 16 point operations. Applying them according to Eq. (6), for the single-site matrix we obtain the simple form

$$A^{(i,i)} = \begin{pmatrix} 0 & 0 & 0 \\ 0 & 0 & 0 \\ 0 & 0 & D_0 \end{pmatrix} \quad (7)$$

where D_0 is the single-site anisotropy parameter. For the interaction matrices between atoms 0 and 1 of the two U layers (Fig. 1) we get

$$A^{(0,1)} = \begin{pmatrix} j_1 - \frac{1}{3}d_1 & b & c \\ b & j_1 - \frac{1}{3}d_1 & c \\ c & c & j_1 + \frac{2}{3}d_1 \end{pmatrix} \quad (8)$$

where j_1 is isotropic exchange parameter, d_1 is two-site anisotropy parameter or, equivalently, anisotropic-exchange parameter, b and c are real numbers. The interaction matrices between atom 0 and atoms 1-4 are transformed to each other by symmetry operations and therefore are determined by the same set of parameters. For atomic pairs (0,2), (0,3) and (0,4) we get, respectively:

$$\begin{pmatrix} j_1 - \frac{1}{3}d_1 & -b & c \\ -b & j_1 - \frac{1}{3}d_1 & -c \\ c & -c & j_1 + \frac{2}{3}d_1 \end{pmatrix}, \begin{pmatrix} j_1 - \frac{1}{3}d_1 & b & -c \\ b & j_1 - \frac{1}{3}d_1 & -c \\ -c & -c & j_1 + \frac{2}{3}d_1 \end{pmatrix}, \begin{pmatrix} j_1 - \frac{1}{3}d_1 & -b & -c \\ -b & j_1 - \frac{1}{3}d_1 & c \\ -c & c & j_1 + \frac{2}{3}d_1 \end{pmatrix}. \quad (9)$$

The same symmetry properties are valid for the interaction matrices between atom 0 and atoms 5-8 of the lower U layer (Fig. 1). While the sets of parameters for the two groups of interaction matrices are not equivalent by symmetry we introduce for atoms 5-8 the notations j_2 and d_2 instead of j_1 and d_1 .

The energies of the four magnetic configurations in terms of the parameters of the interaction matrices take the form

$$\begin{aligned} E(\text{AFM}_Z) &= D_0 - J - \frac{2}{3}D_1 \\ E(\text{AFM}_X) &= -J + \frac{1}{3}D_1 \\ E(\text{FM}_Z) &= D_0 + J + \frac{2}{3}D_1 \\ E(\text{FM}_X) &= J - \frac{1}{3}D_1 \end{aligned} \quad (10)$$

where $J = 4(j_1 + j_2)$ and $D_1 = 4(d_1 + d_2)$.

Equations (10) allow us to uniquely determine parameters J , D_0 , D_1 . They are presented as functions of U_H in Fig. 7(b). The anomalous values at $U_H=0.12$ Ry resulting from the anomalous properties of the energy differences discussed above are not presented. In general, the parameters have comparable scales. Because the dependences of the parameters on U_H are different their relative strength also varies. For example, for $U_H=0$ and $U_H=0.025$ Ry, the single-site anisotropy dominates distinctly. At $U_H=0.1$ Ry, both anisotropy parameters practically coincide. For the upper part of the U_H values lying above the discontinuity region the values of all three interaction parameters are similar. This region is of the main interest for us since here the model reproduces correctly all three fundamental ground state properties: magnetic structure, magnetic easy axis, the value of the magnetic moment. The U_H -dependent relation between the values of the single-site and two-site anisotropies reflects the importance of both single-site and inter-site processes and can be treated as one of the manifestations of the localization-delocalization duality.

3. Zeeman energy and interpretation of experiment

Let us make an estimation of the relevant Zeeman energy. If we take magnetic field of 30 T and the U magnetic moment of $2.5 \mu_B$ we obtain the energy of ~ 0.3 mRy per U atom that is of the same scale as the three other estimated parameters [Fig. 7(b)].

The comparable values of different energy factors explain why large values of the moments are induced for both easy and hard field directions. The induced magnetic configurations are canted magnetic structures with average magnetization parallel to the direction of the field. A schematic presentation of two canted states is given in Fig. 8. The canting means the deviation of the atomic moments from both the ground state AFM structure and the easy c axis. The corresponding energy in-

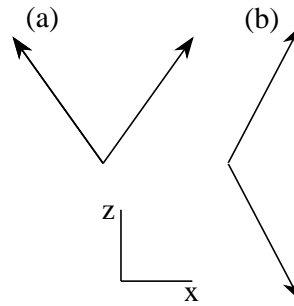


FIG. 8: Schematic presentation of canted magnetic structures in magnetic field parallel to the z axis (a) and x axis (b). In the ground state the the magnetic moments are collinear to the z axis and antiparallel to each other.

crease is compensated by the Zeeman energy of magnetic moments.

The close-to-discontinuity field dependence, i.e. MMT or spin-flop transition, for $B||z$ is the consequence of the MA since the continuous transition of the U moments with negative z projection towards the positive direction of the z axis needs passing the xy plane where the MA energy is high (more about MMT in an AFM can be found in, e.g., Refs. 49–51). For the canting of the moments toward the x axis, such an energy barrier does not appear.

Our interpretation of the in-field experiment is primarily based on the local-moment picture. Of course the presence of the 5f states at the Fermi level contributes to the values of the moments and of the energies of magnetic configurations. The longitudinal scenario of the strong magnetization change seems, however, improbable because the energy cost of the large change of the atomic moment value is much higher than the energy gain from the Zeeman interaction of these moments with external field. For instance, in the GGA calculation the energy difference between AFM_Z and nonmagnetic state is as high as 7.25 mRy/U.

D. Relation between MAE and OMA

We notice that our results violate the relation between MAE and OMA suggested by Bruno²⁵: the easy magnetic direction corresponds to the largest value of the OM. In our calculations, the OM of the AFM_X configuration is for many U_H values larger than the OM of the AFM_Z configuration (Fig. 4) whereas the energy of the AFM_Z configuration is the lowest (Fig. 7). Our next step is to understand the origin of this result in the case of UPS.

The OM appears as a result of the disbalance in the occupation of the orbitals with opposite values of the magnetic quantum number, $\pm m$ -polarization. If the SOC is not taken into account, the occupations of both orbitals are identical and both OM and MAE are zero.

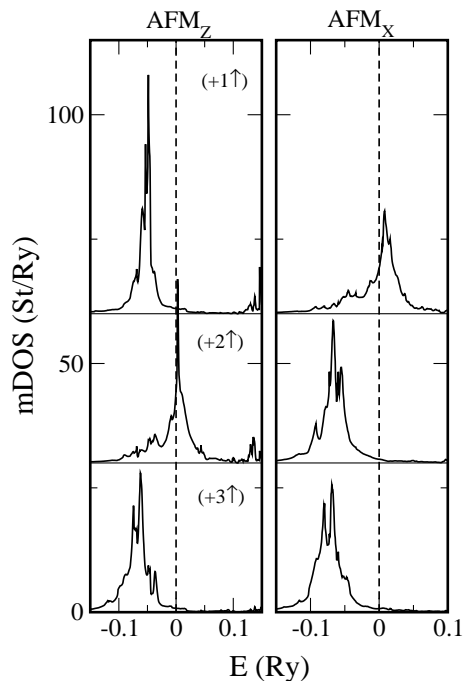


FIG. 9: Comparison of the low-energy mDOSs of the AFM_Z and AFM_X configurations calculated with $U_H=0.1$ Ry.

Because of $\propto \sigma_z l_z$ term, the SOC tends to generate the m -dependent shifts of the 5f orbital energies (see Ref. 52 for full expression of the SOC operator used in the calculations). For negative spin projection one expects the lowest energy position of the $m = 3$ orbital and monotonously increasing energy with decreasing m . The monotonous m -dependence of the energy positions leads to the monotonous variation of the orbital occupations which directly influences the value of the orbital moment. This connection between energies of the orbitals and atomic orbital moment is the physical basis of Bruno's rule.

However, in the calculation for the ground state configuration AFM_Z of UPS we obtained a nonmonotonous m -dependence of the energy positions of the m projected DOSs (see Fig. 9 for $U_H=0.1$ Ry). We connect this result with the hybridization of $m = 3$ and $m = 1$ orbitals that does not allow the intraatomic SOC to split them. The filling of the $m = 1$ orbital instead of the $m = 2$ orbital reduces the value of the OM. This disturbs the straightforward relation between energies of the orbitals and corresponding OM.

Now let us turn to the AFM_X configuration. The mDOSs and m -occupancies for the spherical harmonics defined with respect to the z axis are not helpful for the analysis of the OMs parallel to the x axis. In Fig. 9 we plot mDOSs of AFM_X for the basis of the 5f functions defined with respect to the x axis as quantization axis. In this case we obtain a usual picture: the m -dependence of the energy positions and, therefore, m -occupancies are monotonous with respect to m . We see here the com-

petition between local tendency to the monotonous m -dependence and the influence of the electron delocalization results in dewatering simple relation between MAE and OMA. This is not the first case where the Bruno's relation is not fulfilled⁵³ On the other hand, this relation is operative for numerous materials, also for U compounds (see, e.g., Ref. 5).

E. Relation to the T5FEG-duality model

Our GGA+ U calculations give the results which can be treated as revealing the coexistence of localized and itinerant 5f states supporting the assumption of the T5FEG-duality model. Indeed, in the ground state AFM_Z configuration (Fig. 5) we have two 5f orbitals lying distinctly below E_F while the states related to a third 5f orbital are in the Fermi energy region. We emphasize that this result is obtained applying the same U_H to all 5f orbitals. In the spirit of the T5FEG model it seems plausible to consider a different treatment of the two groups of the 5f orbitals applying the GGA+ U term to only $m = 3$ and $m = 1$ orbitals⁵⁴. In this model calculation we were unable to reach the experimental value of the atomic moment. As seen in Fig. 4, in the U_H interval from 0.1 Ry to 0.2 Ry both spin and orbital moments grow somewhat with increasing U_H . However, these changes mostly compensate each other resulting in the total moment close to $1.5 \mu_B$ for the whole U_H interval, that is distinctly smaller than the experimental value and in strong contrast to the results of the GGA+ U calculations.

To understand this feature we compare the occupation numbers obtained in the T5FEG calculation with those obtained in the standard GGA+ U calculations (Fig.6). The crucial difference in the results of the two calculations is the absence in the T5FEG case of both the discontinuous behavior and fast increase of the occupation number of the $m = 2$ obtained in the GGA+ U calculations. This increase is critical for getting the value of the U moment close to the experimental one. The sum of the occupation numbers for all m and both spin projections is 2.56 for $U_H = 0.1$ Ry and 2.64 for $U_H = 0.1$ Ry what compares well with given above corresponding values from the GGA+ U calculations. (For completeness, in Fig. 11 of Appendix B we compare mDOSs calculated with GGA+ U and in the T5FEG simulation.)

This failure of the modified method is one more signature of the complexity of the multiple-orbital nature of the U 5f electron system in the U based materials. The neglect of the influence of the correlation on the $m = 2$ orbital, contributing to the formation of itinerant electron states, results in the changes in the 5f electron system that does not allow to reach the agreement with experiment.

V. CONCLUSIONS

The paper deals with the U based compound UPS. A wide variation of the properties of the U compounds demands the application of the material specific DFT based methods to their theoretical study. In the case of UPS, the number of such studies is very scarce. In contrast, the experimental data are rich. The goal of this paper is to contribute to filling this gap. We start with identification of the DFT+ U based physical model adequately describing the set of fundamental ground state properties: magnetic structure, magnetic easy axis, the value of the U atomic moment. We demonstrate that the system possesses well formed atomic moments able to participate in transversal magnetic fluctuations.

On this basis the high magnetic field experiment is interpreted. This experiment shows the presence of a strong MMT for the field direction parallel to the easy axis in contrast to the hard direction where such a clear feature is absent. On the other hand, comparable induced magnetization values are obtained for both easy and hard field directions. Within the framework of the suggested model, we interpret this combination of properties as the result of the competition of three energy contributions: exchange energy, MAE, and Zeeman energy. All three energies are estimated and shown to have comparable values.

We notice and discuss the violation in the case of UPS of the Bruno's relation between MAE and OMA for some of the U_H values.

At all steps of the study we devote special attention to revealing and emphasizing the dual itinerant-localized properties of the material. Such an analysis is a useful tool for the in-depth study of the physics of the system. The obtained forms of the duality are different: well defined atomic moments formed by the itinerant electrons, interplay of the single-site and two-site anisotropies, strong localization of two of the 5f electrons in contrast to the itinerant nature of the 5f electrons contributing to the states around the Fermi level, intense Stoner continuum competing with spin wave formation.

The paper contributes to the understanding that the wide range of complex behavior observed in U based materials is the consequence of the multiple-orbital nature of the 5f electron system whose properties are sensitive to numerous factors such as crystal structure, ligand types, intraatomic electron correlation, strength and direction of the applied magnetic field.

The continuation of the study of UPS in the following two directions appears to us of high interest. The first is the numerical investigation of the magnetic excitations by means of material-specific DFT-based calculation of transverse dynamic magnetic susceptibility (see, e.g., Refs. 55–57) aiming at exposing the reason for the absence of the spin waves in the INS experiment¹⁷. A possible reason for the absence of the spin waves is the presence of intensive low-energy Stoner continuum leading to strong damping of the potential spin waves. There

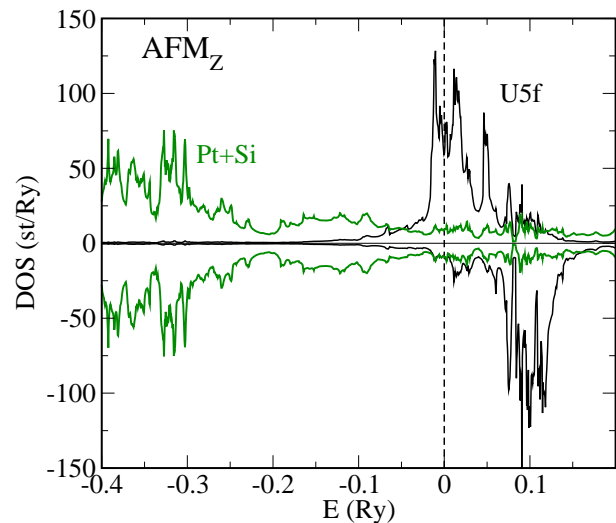


FIG. 10: The U 5f DOS and the sum of the Pt and Si DOSs.

are two factors telling us that such a continuum is expected in UPS. The first is the presence of the electron states corresponding to the U 5f orbitals in the Fermi level region [Fig. 11(d)], both below and above E_F . Second, it is important that the magnetic structure is AFM and all electron bands are double degenerate with pairs of states having equal energies and opposite z projections of the magnetic moments (see, e.g., Ref. 58 for a detailed discussion of the Stoner excitations in an AFM). Therefore, the numerous states participating in the low-energy spin-flip transitions are available. Another feature to remark is the presence of a narrow empty DOS peak close to E_F [Fig. 11(d)]. The electron transitions to this peak build the main part of the Stoner continuum. It would be of high interest to compare theoretical TDMSs for various U compounds with available experimental INS data to obtain a general picture. We should, however, remark that, in the case of the U based materials, the DFT-based calculation of the TDMA is a very complex computational task since it must include a consequent account for both strong SOC and local electron correlation governed by Hubbard parameter U_H .

The second direction is the application of the methods of more advanced account for electron correlation than DFT+ U , in particular of the DFT plus dynamic mean field theory (DFT+DMFT) method⁵⁹. This problem is also numerically very challenging and computer resources demanding.

Appendix A: DOS in a wide energy interval

In Fig. 10 we show the U 5f DOS and the sum of the Pt and Si DOSs of the AFM $_Z$ configuration in a wide energy range. The common structure elements, i.e. common local maxima and minima of the curves, reveal the hybridization of the 5f orbitals and delocalized Pt and Si

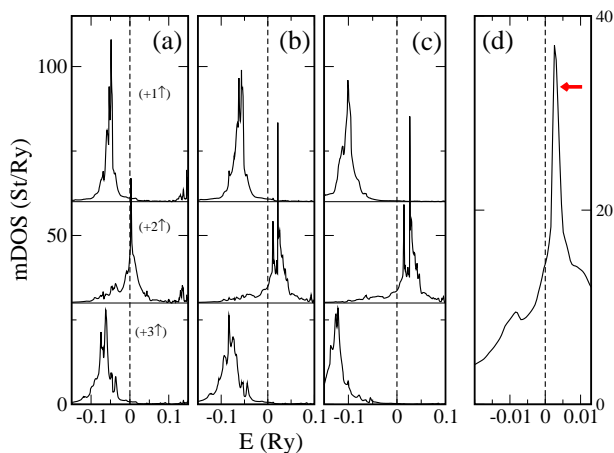


FIG. 11: Panels (a)-(c): Comparison of the low-energy mDOSs of the AFM_Z configuration calculated with the standard GGA+ U method and $U_H=0.1$ Ry (a), and using the GGA+T5FEG modification with $U_H=0.1$ Ry (b) and 0.15 Ry (c). Panel (d): zooming into the Fermi energy region of the $m = 2$ mDOS from panel (a). The arrow in panel (d) marks the mDOS peak that may play important role in the formation of the Stoner continuum.

states. Also in the energy region where the partial DOS of the 5f orbitals is very large, the admixture of the Pt and Si states is important.

Appendix B: Comparison of mDOSs in GGA+ U and T5FEG calculations

In Fig. 11 we present the spin-majority mDOSs for m equal to 3, 2, and 1 obtained in different calculations. Figure 11(a) shows the result of standard GGA+ U calculation with $U_H=0.1$ Ry. Figures 11(b),(c) present the results of the T5FEG-type modification of the method with $U_H=0.1$ Ry and $U_H=0.15$ Ry, respectively.

The comparison of the (a) and (b) panels shows that the application of U_H to only $m = 3$ and $m = 1$ orbitals results in their deeper energy position. and somewhat higher occupations than in the standard case. The trend continues with increasing U_H , Fig. 11(c). The position of the $m = 2$ orbitals with respect to the Fermi level does not change importantly. The corresponding occupation numbers are given in Fig. 4 and discussed in the main text.

- ¹ Physica B **177**, 173 (1992) V. Sechovsky and L. Havela, in *Handbook of Magnetic Materials*, edited by K. H. Bushow (Elsevier, Amsterdam, 1998). p. 1.
- ² P. Santini, Romuald Lemanski, and Paul Erdos, Adv. Phys. **48**, 537 (1999).
- ³ J. A. Mydosh, Adv. Phys. **66**, 263 (2017).
- ⁴ V. Yu. Irkhin and Yu. P. Irkhin, *Electronic Structure, Correlation Effects, and Physical Properties of d- and f-Metals and Their Compounds* (Cambridge International Science, Cambridge, 2007).
- ⁵ Atsushi Miyake, Leonid M. Sandratskii, Ai Nakamura, Fuminori Honda, Yusei Shimizu, Dexin Li, Yoshiya Homma, Masashi Tokunaga, and Dai Aoki, Phys. Rev. B **98**, 174436 (2018).
- ⁶ Larissa Q. Huston, Dmitry Y. Popov, Ashley Weiland, Mitchell M. Bordelon, Priscila F. S. Rosa, Richard L. Rowland, II, Brian L. Scott, Guoyin Shen, Changyong Park, Eric K. Moss, S. M. Thomas, J. D. Thompson, Blake T. Sturtevant, and Eric D. Bauer, Phys. Rev. Materials **6**, 114801 (2022).
- ⁷ Adam P. Pikul, Maria Szlawska, Xiixin Ding, Józef Szajd, Masashi Ohashi, Dorota A. Kowalska, Mathieu Pasturel, and Krzysztof Gofryk, Phys. Rev. Materials **6**, 104408 (2022).
- ⁸ Sara B. Isbill, Ashley E. Shields, J. L. Niedziela, and Andrew J. Miskowiec, Phys. Rev. Materials **6**, 104409 (2022).
- ⁹ Rolando Saniz, Gianguido Baldinozzi, Ine Arts, Dirk Lamoen, Gregory Leinders, and Marc Verwerft, Phys. Rev. Materials **7**, 054410 (2023).
- ¹⁰ Christovam, A. Amorese, Chun-Fu Chang, P. Dolmantis, A.H. Said, H. Gretarsson, B. Keimer, M.W. Haverkort, A.V. Andreev, L. Havela, P. Thalmeier, Liu Hao Tjeng, and A. Severing,
- ¹¹ Andrew D. Huxley, Physica C **514**, 368 (2015).
- ¹² J. A. Mydosh and P. M. Oppeneer, Rev. Mod. Phys. **83**, 1301 (2011).
- ¹³ H. Amitsuka, T. Sakakibara, K. Sugiyama, T. Ikeda, Y. Miyako, M. Date, and A. Yamagishi, Physica B **177**, 173 (1992).
- ¹⁴ S. Elgazzar, J. Ruzs, P. M. Oppeneer, and J. A. Mydosh, Phys. Rev. B **86**, 075104 (2012).
- ¹⁵ D. Schulze-Grachtrup, M. Bleckmann, B. Willenberg, S. Süllow, M. Bartkowiak, Y. Skourski, H. Rakoto, I. Sheikin, and J. A. Mydosh, Phys. Rev. B **85**, 054410 (2012).
- ¹⁶ D. Schulze-Grachtrup, N. Steinki, S. Süllow, Z. Cakir, G. Zwicknagl, Y. Krupko, I. Sheikin, M. Jaime, and J. A. Mydosh, Phys. Rev. B **95**, 134422 (2017).
- ¹⁷ Jooseop Lee, Masaaki Matsuda, John A. Mydosh, Igor Zaliznyak, Alexander I. Kolesnikov, Stefan Süllow, Jacob P. C. Ruff, and Garrett E. Granroth, Phys. Rev. Lett. **121**, 057201 (2018).
- ¹⁸ Valeri Petkov, R. Baumbach, A. M. Milinda Abeykoon, and J. A. Mydosh, Phys. Rev. B **107**, 245101 (2023).
- ¹⁹ S. Süllow, A. Otop, A. Loose, J. Klenke, O. Prokhnenko, R. Feyerherm, R.W.A. Hendrikx, J.A. Mydosh, H. Amitsuka, J. Phys. Soc. Japan **77**, 024708 (2008).
- ²⁰ I. M. Lifshitz, Sov. Phys. JETP **11**, 1130 (1960).
- ²¹ The Lifshitz transition assumes important change of the electron structure in the Fermi energy region.
- ²² O. Eriksson, M. S. S. Brooks, and B. Johansson, Phys. Rev. B **41**, 7311 (1990).
- ²³ V. I. Anisimov, F. Aryasetiawan, and A. I. Lichtenstein, J. Phys.: Cond. Matter **9**, 767 (1997).
- ²⁴ I. V. Solovyev, A. I. Lichtenstein, and K. Terakura, Phys. Rev. Lett. **80**, 5758 (1998).
- ²⁵ P. Bruno, Phys. Rev. B **39**, 865 (1989).
- ²⁶ B. Ujfalussy, L. Szunyogh, P. Bruno, and P. Weinberger, Phys. Rev. Lett. **77**, 1805 (1996).

- ²⁷ Justin M. Shaw, Hans T. Nembach, and T. J. Silva, Phys. Rev. B **87**, 054416 (2013).
- ²⁸ T. Moriya, *Spin Fluctuations in Itinerant Electron Magnetism* (Springer-Verlag, Berlin, 1985).
- ²⁹ B.L.Gyorffy, A.J.Pindor, J.Staunton, G.M.Stocks, and H.Winter, J.Phys.F:Met.Phys. **15**, 1337 (1985).
- ³⁰ J. Kübler, *Theory of Itinerant Electron Magnetism* (Oxford University Press, New York, 2002).
- ³¹ A. I. Liechtenstein, M. I. Katsnelson, V. P. Antropov, and V. A. Gubanov, J. Magn. Magn. Mater. **67**, 65 (1987). Attila Szilva, Yaroslav Kvashnin, Evgeny A. Stepanov, Lars Nordström, Olle Eriksson, Alexander I. Liechtenstein, and Mikhail I. Katsnelson, Rev. Mod. Phys. **95**, 035004 (2023).
- ³² Sergiy Mankovsky and Hubert Ebert, Electron. Struct. **4**, 034004 (2022).
- ³³ I. Turek, J. Kudrnovský, V. Drchal, and P. Bruno, Philosophical Magazine, **86**, 1713 (2006).
- ³⁴ An example of the system where the local moment picture is not applicable is fcc-Cr where the magnetism is of the spin-density-wave type and caused by the nesting features of the Fermi surface: Eric Fawcett, Rev. Mod. Phys. **60**, 209 (1988).
- ³⁵ The discussion of the importance of the duality approach in the case of Fe based superconductors can be found, e.g. in review P. Dai, J. Hu, and E. Dagotto, Nature Phys. **8**, 709 (2012).
- ³⁶ J. G. Zwicknagl, A. Yaresko, and P. Fulde, Phys. Rev. B **68**, 052508 (2003).
- ³⁷ G. Zwicknagl, Rep. Prog. Phys. **79**, 124501 (2016).
- ³⁸ Andrea Amorese, Martin Sundermann, Brett Leedahl, Andrea Marino, Daisuke Takegami, Hlynur Gretarsson, Andrei Gloskovskii, Christoph Schlueter, Maurits W Haverkort, Yingkai Huang, Maria Szlawaska, Dariusz Kaczorowski, Sheng Ran, M Brian Maple, Eric D Bauer, Andreas Leithe-Jasper, Philipp Hansmann, Peter Thalmeier, Liu Hao Tjeng, Andrea Severing, PNAS **117**, 30220 (2020).
- ³⁹ A. R. Williams, J. Kübler, and C. D. Gelatt, Phys. Rev. B **19**, 6094 (1979).
- ⁴⁰ V. Eyert, *The Augmented Spherical Wave Method, Lecture Notes in Physics* **849**, (Springer-Verlag Berlin Heidelberg 2012).
- ⁴¹ L. M. Sandratskii, Adv. Phys. **47**, 91 (1998).
- ⁴² J. P. Perdew, K. Burke, and M. Ernzerhof, Phys. Rev. Lett. **77**, 3865 (1996).
- ⁴³ S. L. Dudarev, G. A. Botton, S. Y. Savrasov, C. J. Humphreys, and A. P. Sutton, Phys. Rev. B **57**, 1505 (1998).
- ⁴⁴ L. M. Sandratskii and K. Carva, Phys. Rev. B **103**, 214451 (2021).
- ⁴⁵ L. M. Sandratskii, V. M. Silkin, and L. Havela, Phys. Rev. Materials **7**, 024414 (2023).
- ⁴⁶ In the ASW calculation, the electron occupation numbers appear as a result of the mathematical procedure consisting of the evaluation of the contributions of certain spherical harmonics in the decomposition of the crystal wave functions in the U atomic area. The atom-centered basis functions, augmented spherical waves, used in the method are complex constructs treating differently the atomic region of the central atom, the atomic regions of other atoms, and the interstitial region. As a result, for the U atom there are two different radial wave functions with $l = 3$ contributing to the decomposition of the crystal wave functions: one corresponding to the central atom (Hankel-type function) and the other obtained through the augmentation to the tails of the basis functions centered at other atoms (Bessel-type function). In Fig. 6, we show the central-atom type contribution.
- ⁴⁷ The interplay of the exchange interaction, single-site anisotropy and anisotropic exchange interaction is an important effect not only for the U based compounds. See, e.g., a recent publication on two-dimensional 3d-atoms based magnets: F. Delgado, M. M. Otrokov, A Arnau, arXiv:2310.15942.
- ⁴⁸ L. M. Sandratskii, Phys. Rev. B **94**, 184414 (2016).
- ⁴⁹ A. N. Bogdanov, A. V. Zhuravlev, and U. K. Rößler, Phys. Rev. B **75**, 094425 (2007).
- ⁵⁰ Bastien Leclercq, Houria Kabbour, Françoise Damay, Claire V. Colin, Alain Pautrat, Angel M. Arevalo-Lopez, and Olivier Mentre, Inorg. Chem. **58**,12609 (2019).
- ⁵¹ Jun Zhao, Azizur Rahman, Wei Liu, Fanying Meng, Langsheng Ling, Yuyan Han, Chuanying Xi, Wei Tong, Longmeng Xu, Zhaoming Tian, Li Pi, Lei Zhang, and Yuheng Zhang Phys. Rev. B **106**, 224412 (2022).
- ⁵² L. M. Sandratskii, Phys. Rev. B **96**, 024450 (2017).
- ⁵³ C. Andersson, B. Sanyal, O. Eriksson, L. Nordström, O. Karis, D. Arvanitis, T. Konishi, E. Holub-Krappe, and J. Hunter Dunn, Phys. Rev. Lett. **99**, 177207 (2007).
- ⁵⁴ This means that matrix element $n_{m,m'}$ is set to zero if either m or m' differs from 1 and 3.
- ⁵⁵ P. Buczek, A. Ernst, and L. M. Sandratskii, Phys. Rev. B **84**, 174418 (2011).
- ⁵⁶ Samir Lounis, Manuel dos Santos Dias, and Benedikt Schweflinghaus, Phys. Rev. B **91**, 104420 (2015).
- ⁵⁷ T Skovhus and T Olsen, Phys. Rev. B **103**, 245110 (2021).
- ⁵⁸ Leonid M. Sandratskii and Pawel Buczek, Phys. Rev. B **85**, 020406(R) (2012).
- ⁵⁹ G. Kotliar, S. Y. Savrasov, K. Haule, V. S. Oudovenko, O. Parcollet and C. A. Marianetti, Rev. Mod. Phys. **78**, 865 (2006).